





RESEARCH ARTICLE

OPEN ACCESS

HEAT TRANSFER ENHANCEMENT IN A P-SHAPE FINNED RADIAL HEAT SINK SUBJECTED TO NATURAL CONVECTION: THERMAL SIGNIFICANCE OF SLOT AND DIMPLES IN FIN

Ibrahim Fetuga*¹, T. Olabode Olakoyejo², O. Adekunle Adelaja³ and K. Joshua Gbegudu⁴

^{1, 2, 3, 4} Department of Mechanical Engineering, University of Lagos – Akoka, Yaba-Lagos, Nigeria.

¹ <http://orcid.org/0000-0002-1943-4234> , ² <http://orcid.org/0000-0001-9942-1339> , ³ <http://orcid.org/0000-0001-9175-8332> ,
⁴ <http://orcid.org/0000-0003-2417-2520> 

Email: *fetugaebraheem@gmail.com, oolakoyejo@unilag.edu.ng, aadelaja@unilag.edu.ng, jk.gbegudu@gmail.com

ARTICLE INFO

Article History

Received: March 05th, 2022

Accepted: April 24th, 2022

Published: April 30th, 2022

Keywords:

Radial heat sink,
P-shape fin,
Slot,
Dimples,
Natural convection.

ABSTRACT

This study presents the optimum design of the radial heat sink for light-emitting diode (LED) under natural convection. A radial heat sink with a hollow circular base and a P-shape fin type incorporated with either slots or both slots and dimples was numerically investigated using the ANSYS (Fluent) commercial code, with the aim of achieving better cooling performance at a lower heat sink mass. The average temperature (T_{avg}) and mass of the HS for various model designs, namely; Type A (HS with plain fin), Type B (HS with slot) and Type C (HS with both dimples and slot) were compared to select the best configuration. The effect of heat flux ($700 \leq \dot{q} \leq 1900$) on average temperature of radial heat sink was investigated. It was found that for all three models, the temperature difference between the HS and the ambient air of the fluid domain linearly increased with heat flux. At $\dot{q} = 1900 \text{ W/m}^2$, when compared to Type A (HS with plain fins), Type C (HS with slot and dimples) models offered the best cooling performance, followed by Type B where the mass and average temperature of the heat sink is reduced by 13.7% and 5.1%, 8.3% and 1%, respectively.



Copyright ©2022 by authors and Galileo Institute of Technology and Education of the Amazon (ITEGAM). This work is licensed under the Creative Commons Attribution International License (CC BY 4.0).

I. INTRODUCTION

Cooling through free convection is suitable, especially for small electronics components such as LEDs because it is relatively simple, less expensive and eco- friendly. LED is known for its durability, efficiency, and cost-effectiveness. Thus, LEDs replaced much extant lighting devices. Studies have revealed that more than 50% of the power required by LEDs is transformed into heat. Therefore, it is important to sufficiently cool the LED device for smooth operation and higher efficiency. Cooling of the electronics component may be active or passive, the most widely used device for passive cooling is the heat sink. To meet the demands of higher thermal performance for LED devices, the challenges of cumbersome heat sinks are always encountered. Therefore, cutting-edge technology, perhaps in the aspect of heat sink design, materials selection, mass reduction, and as such, is required to improve the heat sink's performance.

II. THEORETICAL REFERENCE

Several studies have been conducted on the cooling performance of the HS for LED devices. Costa and Lopes [1] used ANSYS (CFX) commercial codes to conduct a computational study on a radial HS having protruded fins under free convection. They revealed that the average temperature of the HS is insignificantly influenced by the thickness of the fin. Furthermore, it was pointed out that the heat sinks average temperature initially declined, and then increased with the number of fins. Jang et al. [2] numerically performed a parametric study on the arrays of pin fins at various height configurations. They observed that the HS with the tallest outermost fin yielded the optimum cooling performance. Sparrow and Vemuri [3] evaluated the heat transfer characteristics of a pin-fin heat sink for several orientations of the installation under the conditions of radiation and natural convection. They found that the vertical pin-fin provided the best cooling

performance. Yildiz and Yuncu [4] demonstrated a study on the thermal performance (TP) of an annular fin mounted on a cylinder subjected to natural convection. They indicated that the highest heat transfer coefficient (HTC) is obtained at an optimum spacing between the fins. Tijani and Jaffri [5] observed the influence of perforations on pin-fin HS subjected to force convection. They concluded that the HTC is improved by 40% in a HS with perforated fins. Jaffal [6] performed both experimental and numerical studies on the TP of HS having different fin designs. He concluded that heat flux strongly influences the heat transfer rate and, more so, HS with perforated fins performed better than others. Rath et al. [7] numerically examined the thermal characteristics of radial HS consisting of longitudinal corrugated fin with three different number of cycles (one cycle, two cycles, and three cycles). They revealed that the highest value of fin effectiveness and Nusselt number was obtained in corrugated fins with three cycles, followed by two cycles and one cycle. Tehmina et al. [8] adopted a multiphase Eulerian-Lagrangian model to simulate the hydrothermal behavior of three different multiwalled carbon nanotubes (MWCNT) heat sinks with hydrofoil pin-fin, rhombus pin-fin, and triangular pin-fin, respectively. They concluded that better performance was achieved in the triangular pin-fin MWCNT heat sink as compared to others. Rahul et al. [9] numerically explored the heat transfer enhancement in HS with branched and interrupted fins. They reported that HS with branched fins yielded better performance, and they further suggested that higher performance is obtained in HS with branched fins when the symmetrically oriented secondary fins of the branched fins are far from the base of the plate. Ding et al. [10] carried out experimental and numerical studies on the thermal dissipation behaviors of vertically oriented finned tubes. They indicated that a Nusselt number of about 207% was obtained in a heat sink with finned tubes as compared to that of a convective heat sink. Furthermore, they opined that the effects of circular fin pitch and the width of the fin were insignificant. Hithaish et al. [11] numerically analyzed the hydrothermal characteristics of heat sink with triangular pin-fin at different orientations (30°C to 60°C), height of the fin (0.25mm - 0.75mm) and arrangements (alternate backward and forward). They revealed that HS with triangular pin fins in alternate forward and backward configuration had the highest value of the thermal performance index. In this study, the P-shape fin designs are proposed to enhance the thermal dissipation of the radial heat sink without altering the mass of the HS above the comparable convective HS. Cooling performance of three different HSs (the Type A-HS with plain fin, the Type B-HS with slot, and Type C-HS with both slot and dimples) are compared.

III. METHODOLOGY

III.1 GEOMETRY DESCRIPTION

A three-dimensional HS is designed using Design Modeler of ANSYS (Fluent) software package. Fig. 1(a)-(c) shows three different designs of radial heat sink, Type A-plain, Type B-slot and Type C-slot and dimples) respectively. Each of the heat sink which made of aluminum material consists of P-shape fins attached to vertically projected annular cylinder and then mounted on hollow circular base. The fins are radially arranged at an equal interval on a hollow circular base which projected horizontally. The bottom of the HS is subjected to heat flux varied from $700\text{W}/\text{m}^2$ to $1900\text{W}/\text{m}^2$, ambient temperature of the air is maintained at 300K . Fig. 2(a)-(b) illustrates the schematic diagram of the fin and computational domain. A portion of the HS containing one fin is demonstrated because of the time consumption as a result of large

number of grids in the simulation. The details of the computational domain and the heat sink parameter are presented in Table 1.

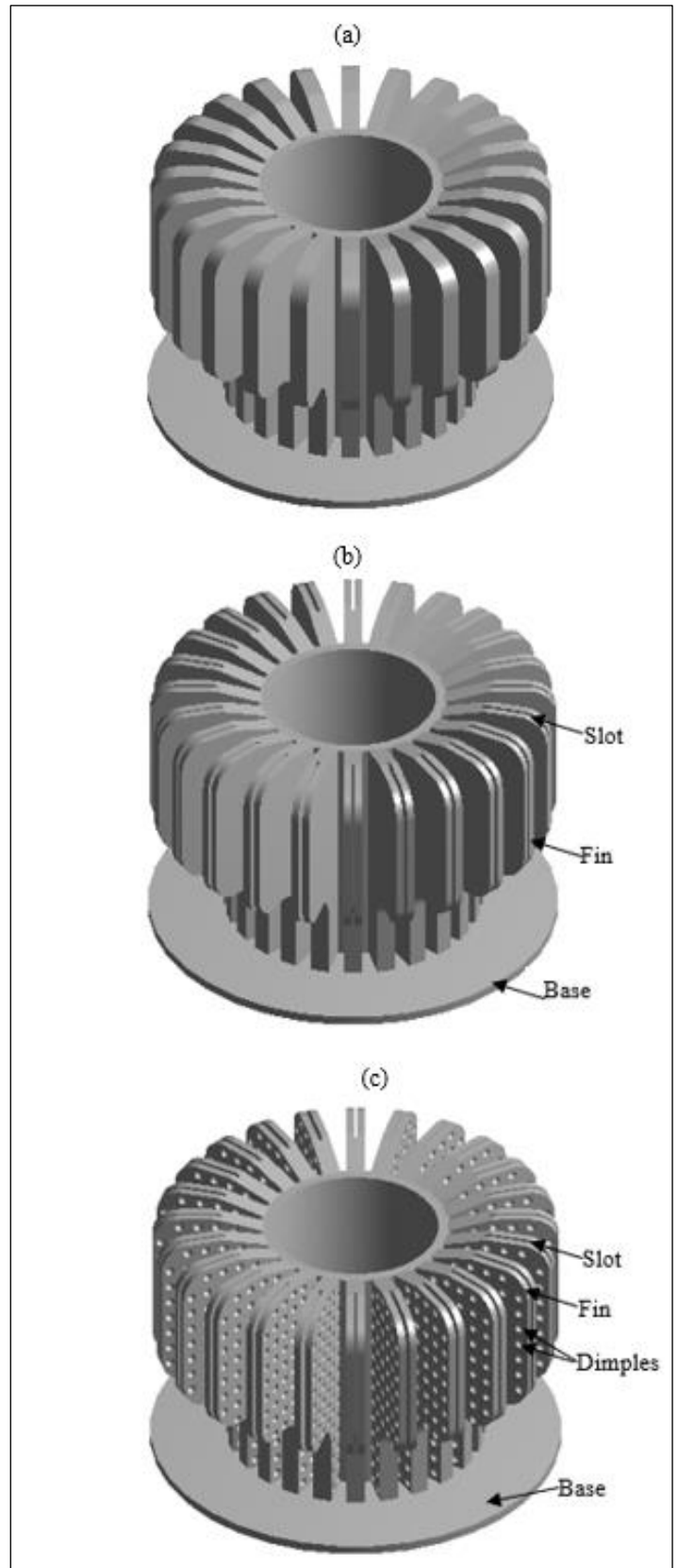


Figure 1: SS (a) Type A (Radial HS with plain fins or convective) (b) Type B (HS with slotted fins) (c) Type C (HS with slotted and dimpled fins).

Source: Authors, (2022).

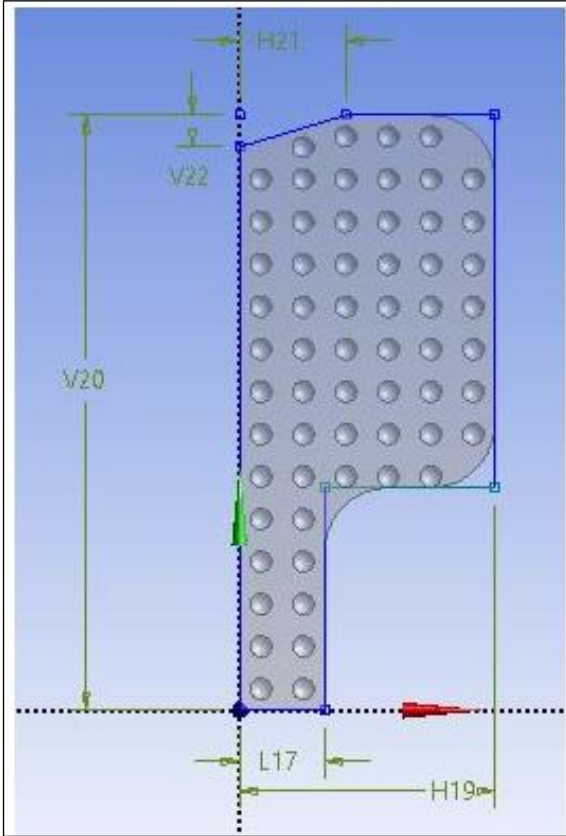


Figure: 2(a) Schematic representation of the fin with dimples.
Source: Authors, (2022).

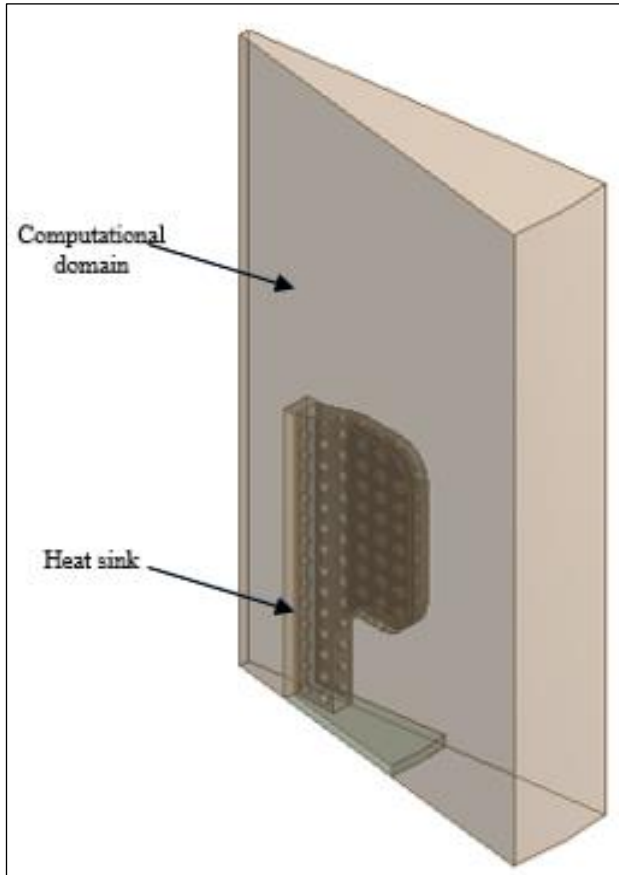


Figure: 2(b) Schematic diagram of the computational domain and HS.
Source: Authors, (2022).

Table 1: Dimensions of the heat sink.

Item	Parameter	Value
Computational domain	Base radius (R)	37.5mm
	Height (H)	145mm
Radial Heat sink		
Circular base	Inner radius (r_i)	9mm
	Outer radius (r_o)	22.25mm
	Base thickness (t_b)	1mm
P-shape Fin	Fin thickness (t_f)	2mm
	H_{19}	12mm
	H_{21}	5mm
	L_{17}	4mm
	V_{20}	28mm
	V_{22}	1.5mm
	Fillet radius (r_f)	2.5mm
	Sphere/Dimple radius (r_D)	0.5mm
	Dimples spacing	2mm
	Slot length (L_s)	7.5mm
	Slot width (W_s)	0.2mm
	Slot height (H_s)	16mm
	Number of fins (N_f)	24

Source: Authors, (2022).

III.2 MESH GENERATION

The grids were generated using ANSYS Mesh. As depicted in Fig. 3(a)-(b), the Qua/Tri hexahedral method was assigned to the whole geometry, while the refined mesh of element size of 0.008mm and 0.009 are assigned to the HS and fluid domain respectively.

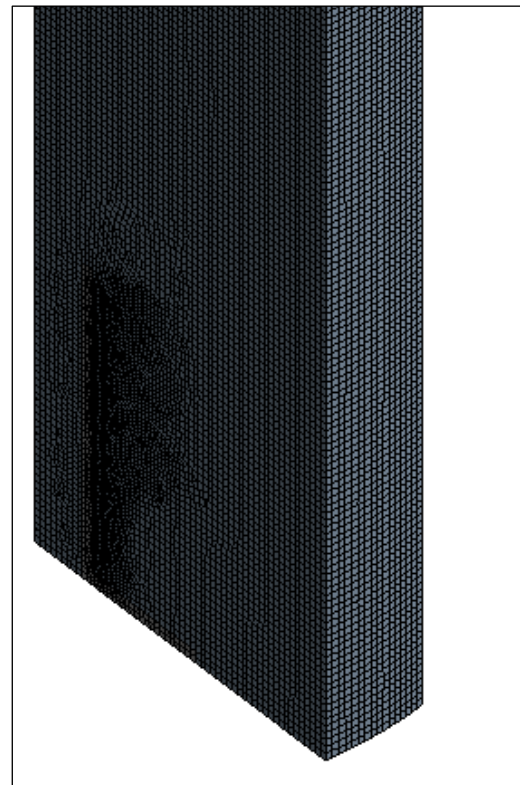


Figure: 3(a) hexahedral grids for computation domain.
Source: Authors, (2022).

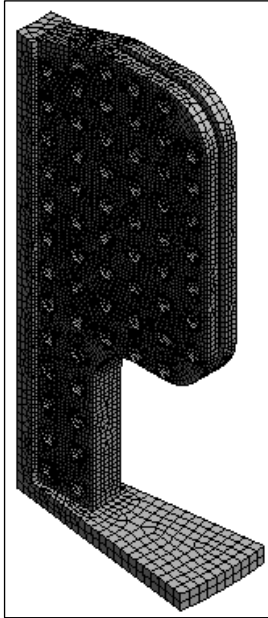


Figure: 3(b) hexahedral grids for heat sink.
Source: Authors, (2022).

III.3 PROBLEM FORMULATION

The computational simulation of natural convection is based on the assumptions stated below.

1. The flow is assumed to be steady, laminal, and three-dimensional.

2. All the properties of air do not depend on the temperature, except the density.
 3. The density of the air is computed by using an ideal gas law.
 4. Radiation and magnetic effects are neglected.
- The governing equations are presented below;

Continuity equation

$$\nabla \cdot (\rho \mathbf{v}) = 0 \quad (1)$$

Momentum equation

$$\frac{D\mathbf{v}}{Dt} = -\frac{\nabla P}{\rho} + \nu \nabla^2 \mathbf{v} - g_y \quad (2)$$

Energy equation

$$\rho C_p \frac{DT}{Dt} = \nabla \cdot (k \nabla T) + \frac{DP}{Dt} \quad (3)$$

Ideal gas law is used to compute density of the air

$$\rho = \frac{p_{atm}}{(R/M_w)T} \quad (4)$$

M_w denotes the molecular weight of the air, which is taken as 28.966 kg/kmol.

The material properties of the heat sink and the boundary conditions adopted for this study are presented in Table 2 and Table 3, respectively.

Table 2: Boundary conditions.

Domain	Location	Hydrodynamic conditions	Thermal conditions
Fluid	Periodic	$u_i(\vec{r}_l) = u_i(\vec{r}_l + \vec{L})$	$T(\vec{r}_l) = T(\vec{r}_l + \vec{L})$
		$\nabla p(x_i) = \eta \frac{\vec{L}}{ \vec{L} } + \nabla p^*(x_i)$	
	Outer	Pressure inlet/Pressure Outlet condition	$T_{inlet} = T_{outlet,backflow} = T_\infty$
Solid	Heat sink base	$u_i = 0$	$-k_s \frac{\partial T_s}{\partial n} = \dot{q}$
	Symmetric face	$u_i = 0$	$\frac{\partial T_s}{\partial n} = 0$
Fluid-solid	Interface	$u_i = 0$	$T_{f,wall} = T_{s,wall}$ $-k_f \frac{\partial T_f}{\partial n} _{wall} + \dot{q}_{out} = -k_s \frac{\partial T_s}{\partial n} _{wall} + \dot{q}_{in}$

Source: Authors, (2022).

Table 3: Thermo-physical properties of the heat sink and the air.

Materials	C_p ($Jkg^{-1}K^{-1}$)	μ ($Pa.s$)	k ($Wm^{-1}K^{-1}$)	ρ (kgm^{-3})
Air	1005	1.834e-05	0.0242	$\frac{p_{atm}}{(R/M_w)T}$
Heat sink	871	-	136.8	2719

Source: Authors, (2022).

III.4 NUMERICAL PROCEDURE

The ANSYS (Fluent) software package was used to perform the numerical simulation, and was used to solve the continuity, Navier-Stokes equations (momentum and energy equation) taking into account the boundary conditions and assumptions stated earlier. The COUPLE Algorithm was assigned for pressure-velocity coupling, default value of under-relaxation parameter was

used, the Least Square cell based was assigned for the gradient under spatial discretization and the second-order upwind scheme was used for density, momentum, and energy, whilst Body Force Weighted was set for pressure. All solver residuals were set to convergence criteria of 1×10^{-4} .

IV. RESULTS AND DISCUSSIONS

To select the best design, we compared the average temperature of all the cases while maintaining the same conditions.

IV.1 GRID SENSITIVITY STUDY

The grid sensitivity test was carried out by increasing the number of grids from 80000 to 600000. The parameters of type A profiles (heat sink with plain fin) at heat flux of $700W/m^2$ are used as reference. As illustrated in Fig. 4, 328221 grid was selected as a

reference grid point from the grid independence test, because a further increase in the number of grid points beyond 328221, yielded less than 2% in the variation of average temperature of the heat sink.

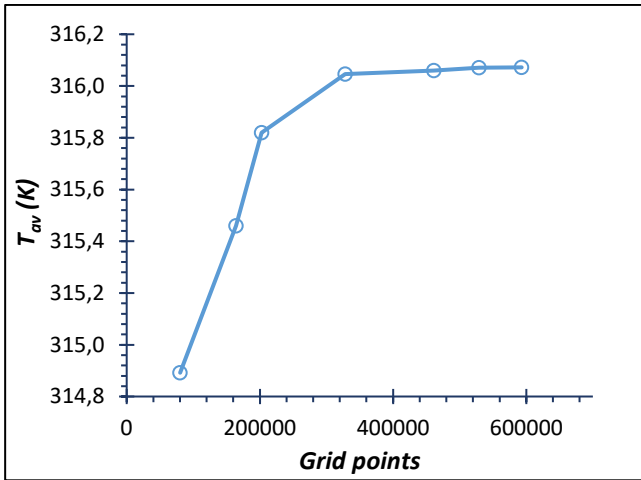


Figure 4: Average temperature of the HS at various grid points. Source: Authors, (2022).

IV.2 MODEL VALIDATION

The difference between the average temperature (T_{avg}) of the HS and the ambient temperature of the air (T_{amb}) is presented to compare the numerical results of this study with the experimental data of Seung-Hwan et al. [12]. The geometry parameters used for validation are $N_f = 20$, $L_f = 55\text{mm}$, $t_f = 2\text{mm}$, $h_{fL} = 21.3\text{mm}$, $h_{fH} = 21.3\text{mm}$, $r_i = 10\text{mm}$, $r_o = 75\text{mm}$, $t_b = 1.5\text{mm}$ and $200 \leq \dot{q} \leq 850$. Fig. 5 presents the comparison of the temperature difference against the heat flux for the numerical results of this work and the experimental data provided by Seung-Hwan et al. [12]. A good agreement is established between the present work and the experimental data of Seung-Hwan et al. [12].

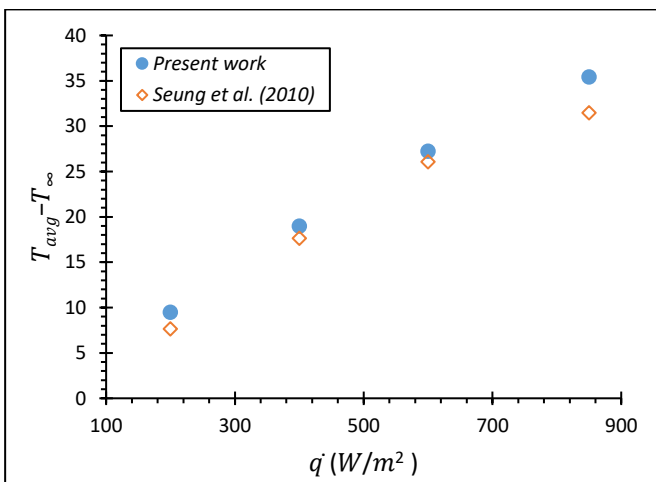


Figure 5: Comparison of temperature difference between the numerical results and experimental result. Source: Authors, (2022).

IV.3 RESIDUALS PLOT

The residuals plot in Fig. 6 below depicts the convergence of the continuity, momentum (velocity) and energy curve for Type A heat sink model at a constant heat flux of $700\text{W}/\text{m}^2$.

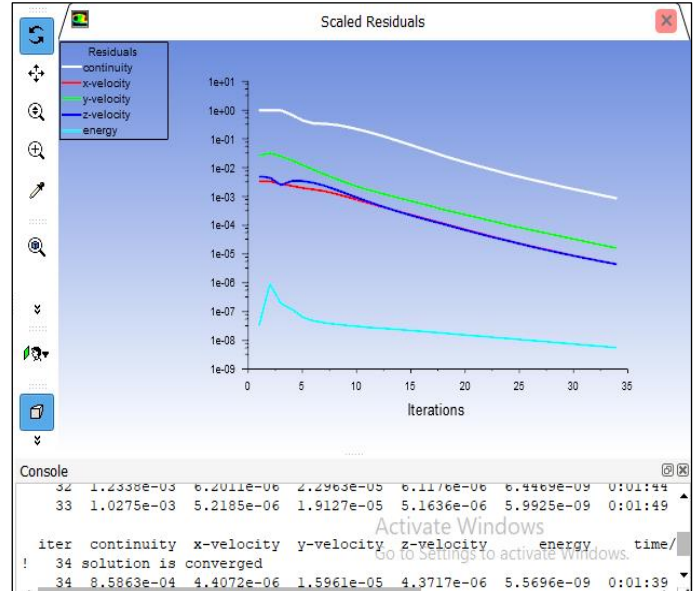


Figure 6: Residuals plot. Source: Authors, (2022).

IV.3 EFFECT OF HEAT FLUX (\dot{q})

Fig. 7 depicts the influence of heat flux applied to the base of a HS on the thermal performance of various model designs. As shown in Fig. 7, the difference between the T_{avg} of the HS and ambient air (T_{amb}) increases linearly with heat flux. At $700 \leq \dot{q} \leq 1900$, Type C (HS with slot and dimples) has lowest temperature difference, followed by Type B (HS with only slot) and Type A (plain). At $\dot{q} = 700\text{W}/\text{m}^2$, temperature difference of 16.05K, 15.12K and 9.83K is reported in Type A (plain), Type B (HS with slot) and Type C (HS with slot and dimples) as follows. However, at $\dot{q} = 1900\text{W}/\text{m}^2$, Type A, Type B and Type C has a temperature difference of 44.48K, 41.7K and 27.05K as followed.

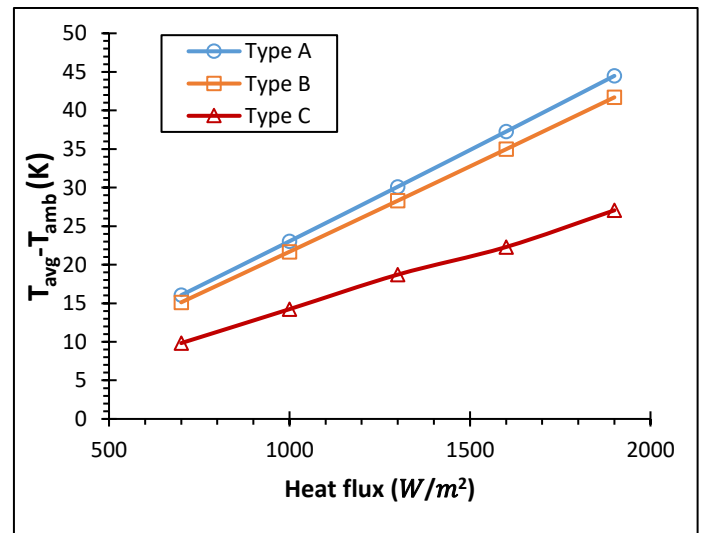


Figure 8: Comparison of temperature difference against heat flux at different model designs. Source: Authors, (2022).

IV.4 COMPARISON OF THE TYPE A (PLAIN), TYPE B (HS WITH) AND TYPE C (HS WITH SLOT AND DIMPLES) MODEL

Table 4 compares the average temperature and mass of each of the HS designs at a constant heat flux of $1900\text{W}/\text{m}^2$. In respect

to Type-A (Plain) HS design, which has the highest average temperature of 344.48K and a mass of 0.00168kg, it is observed that by incorporating a slot in the fin as we have in Type-B HS model, the average heat sink temperature and the mass are reduced by 2.78K and 8.33%, whereas total surface area increases by 29.58%. This simply means that the Type B model has a better thermal performance than the Type A model with just a plain fin, because the slot in Type B creates an additional passage or spacing in the fin which increases the cooling region or heat transfer area of the fin. However, upon the incorporation of both slots and

dimples to the plain fin, as it is shown in Type C model, the T_{avg} and the mass of the HS are decreased by 17.43K and 13.69%. Among all the model designs, Type C (slot and dimples) has been seen to have the best cooling performance and lowest mass. The reason for this is that the incorporation of both slot and dimples has a greater influence on thermal performance by increasing the heat transfer area as compared to the Type B model (HS with slot) and the Type A model with a plain fin.

Table 4: Average Temperature and mass for various heat sink designs at $\dot{q} = 1900 W/m^2$.

Model	Total Area (mm ²)	Frontal Area (mm ²)	Volume (mm ³)	Mass (kg)	Temp (K)
Type A	852.87	287.56	618.31	0.00168	344.48
Type B	1105.2	287.56	566.90	0.00154	341.70
Type C	1201.1	269.5	534.96	0.00145	327.05

Source: Authors, (2022).

IV.4 TEMPERARURE CONTOUR

Fig. 9 through Fig. 11 visualizes the heat flow between the heat sink and fluid domain in the z-x plane and the x-y plane. Heat flows in two directions, which are horizontal direction and upward direction. Heat flows in a horizontal direction when the cooled air from the fluid domain horizontally approaches the outer part of the heat sink where it becomes warmer (the temperature of the cooled air from the fluid domain gradually increases while approaching the outer part of the heat sink). It is also observed that the temperature of the air in the outer part of the HS is comparatively lower than the temperature in the inner part. Furthermore, the

warmed air from the outer part of the HS enters the spaces between the fins and becomes warmer and lighter as compared to its previous state in the outer part. Due to the fact that the surrounding air in the outer part of the HS is heavier than the warmed air between the fins (which has a higher temperature), density therefore plays a greater role here by displacing the warmed air between the fins upward in a vertical direction from the inner part of the HS. However, the temperature of the HS decreases as the cooling air flows from the base to the tip of the HS (the HS which is maintained at a relatively higher temperature, is cooled by the cooling air).

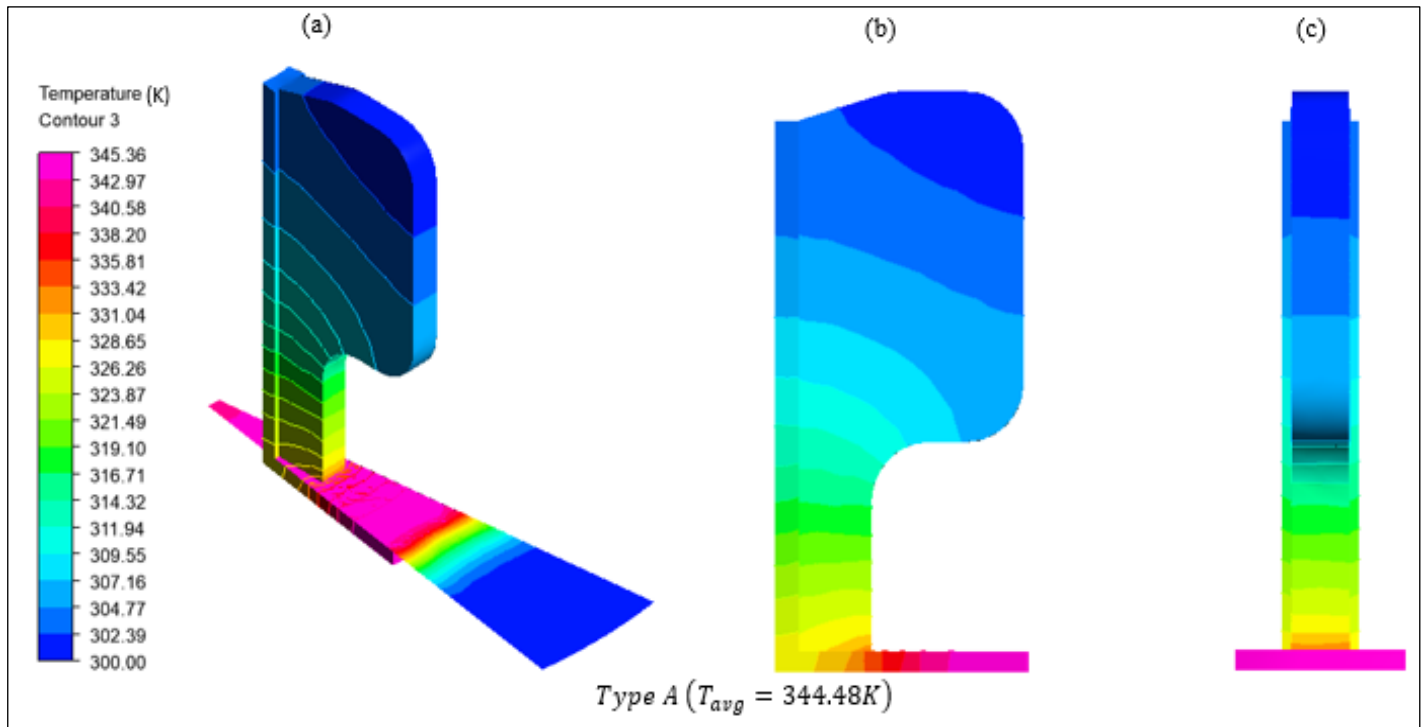


Figure 9: Temperature contour plot of the Type A radial HS at $\dot{q} = 1900 W/m^2$ for (a) 3D view of Type A (b) Side view of Type A (c) Frontal view of Type A. Source: Authors, (2022).

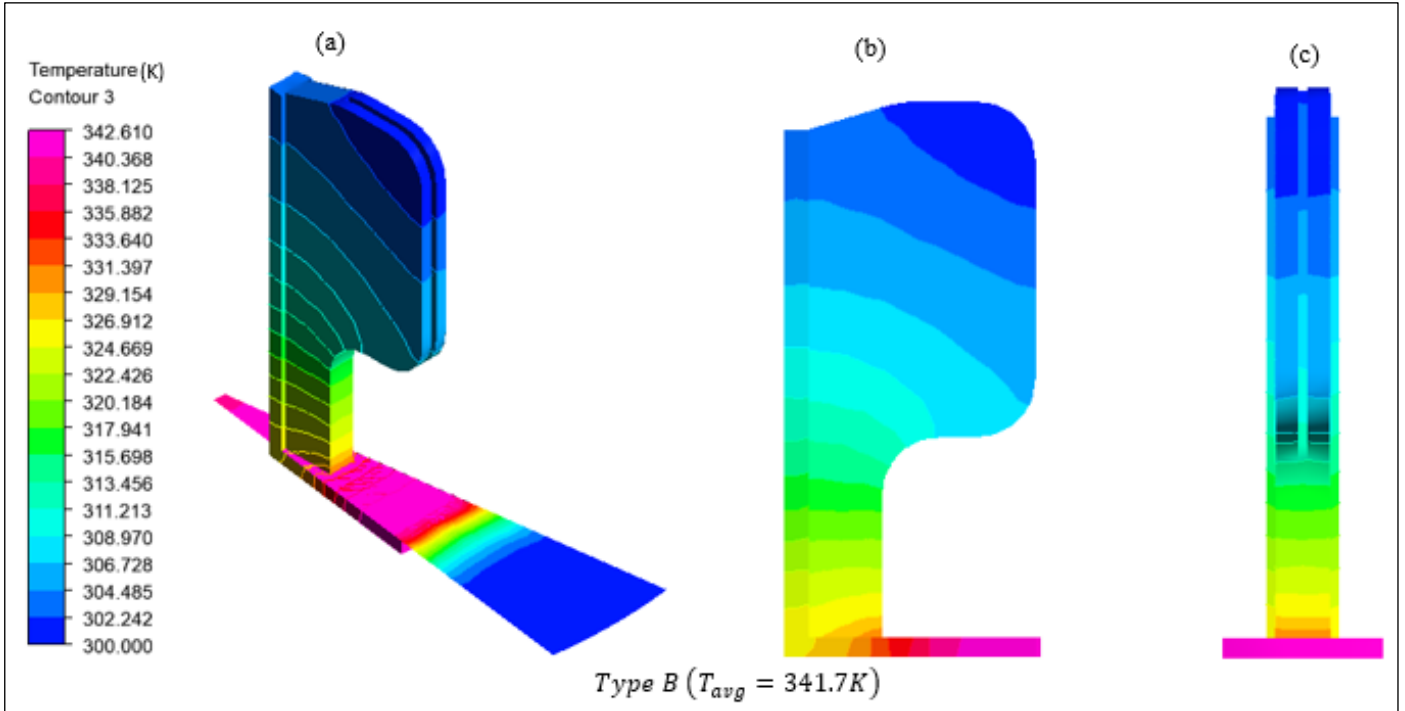


Figure 10: Temperature contour plot of the Type B radial HS at $\dot{q} = 1900 \text{ W/m}^2$ for (a) 3D view of Type B (b) Side view of Type B (c) Frontal view of Type B. Source: Authors, (2022).

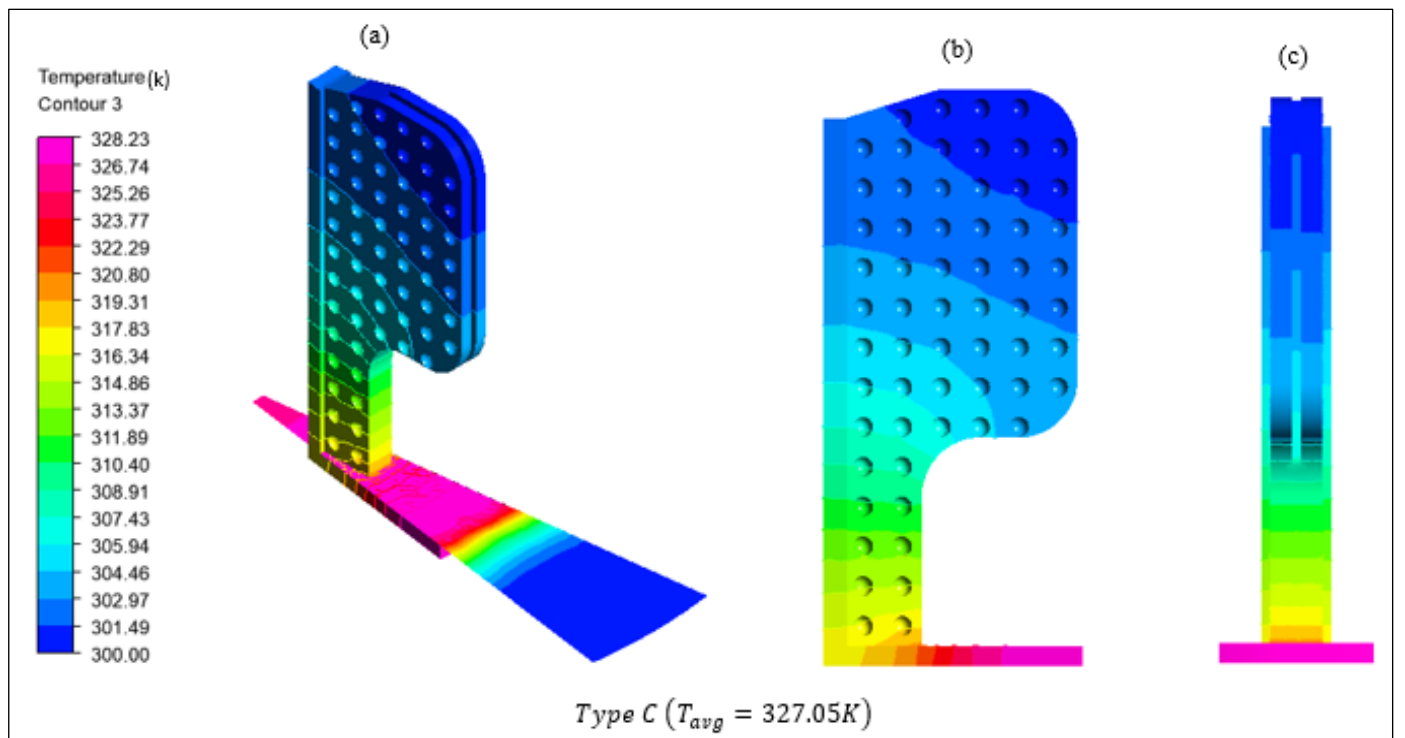


Figure 11: Temperature contour plot of the Type C radial HS at $\dot{q} = 1900 \text{ W/m}^2$ for (a) 3D view of Type C (b) Side view of Type C (c) Frontal view of Type C. Source: Authors, (2022).

V. CONCLUSIONS

Thermal analyses were conducted to maximize the performance of a P-shape finned radial HS under natural convection by using ANSYS (Fluent) software. Validation was carried out by comparing the numerical results with the available experimental data, and the agreement was satisfactory. To

determine the best design for the P-shape finned heat sink, three different designs of heat sink, namely Type A (HS with plain fin), Type B (HS with slot) and Type C (HS with slot and dimples) were compared based on the T_{avg} and mass of the HS. Among all these models, Type C is the most economical and provides the best cooling performance because of its lowest average temperature and heat sink mass.

VI. AUTHOR'S CONTRIBUTION

Conceptualization: A. Ibrahim Fetuga, T. Olabode Olakoyejo, and K. Joshua Gbegudu.

Methodology: A. Ibrahim Fetuga and T. Olabode Olakoyejo.

Investigation: A. Ibrahim Fetuga and O. Adekunle Adelaja.

Discussion of results: A. Ibrahim Fetuga, T. Olabode Olakoyejo and O. Adekunle Adelaja.

Writing – Original Draft: A. Ibrahim Fetuga and K. Joshua Gbegudu.

Writing – Review and Editing: A. Ibrahim Fetuga, T. Olabode Olakoyejo and O. Adekunle Adelaja.

Resources: T. Olabode Olakoyejo.

Supervision: T. Olabode Olakoyejo and O. Adekunle Adelaja.

Approval of the final text: T. Olabode Olakoyejo and O. Adekunle Adelaja.

[12] S. H. Yu, K. S. Lee, and S. J. Yook, "Natural convection around a radial heat sink," *Int. J. Heat Mass Transf.*, vol. 53, no. 13–14, pp. 2935–2938, Jun. 2010, doi: 10.1016/j.ijheatmasstransfer.2010.02.032.

VII. ACKNOWLEDGMENTS

We appreciate the support of university of Lagos for this research.

VIII. REFERENCES

- [1] V. A. F. Costa and A. M. G. Lopes, "Improved radial heat sink for led lamp cooling," *Appl. Therm. Eng.*, vol. 70, no. 1, pp. 131–138, 2014, doi: 10.1016/j.applthermaleng.2014.04.068.
- [2] D. Jang, S. J. Yook, and K. S. Lee, "Optimum design of a radial heat sink with a fin-height profile for high-power LED lighting applications," *Appl. Energy*, vol. 116, pp. 260–268, 2014, doi: 10.1016/j.apenergy.2013.11.063.
- [3] E. M. Sparrow and S. B. Vemuri, "Orientation effects on natural convection/radiation heat transfer from pin-fin arrays," *Int. J. Heat Mass Transf.*, vol. 29, no. 3, pp. 359–368, 1986, doi: 10.1016/0017-9310(86)90206-1.
- [4] Ş. Yildiz and H. Yüncü, "An experimental investigation on performance of annular fins on a horizontal cylinder in free convection heat transfer," *Heat Mass Transf. und Stoffuebertragung*, vol. 40, no. 3–4, pp. 239–251, 2004, doi: 10.1007/s00231-002-0404-x.
- [5] A. S. Tijani and N. B. Jaffri, "Thermal analysis of perforated pin-fins heat sink under forced convection condition," in *Procedia Manufacturing*, 2018, vol. 24, pp. 290–298, doi: 10.1016/j.promfg.2018.06.025.
- [6] J. Hayder Mohammad, "The Effect of Fin Design on Thermal Performance of Heat Sink | Journal of Engineering," *J. Eng.*, vol. 23, no. 5, pp. 123–146, 2017, Accessed: Mar. 04, 2022. [Online]. Available: <https://www.joe.uobaghdad.edu.iq/index.php/main/article/view/45>.
- [7] S. Rath, Siddhartha, and S. K. Dash, "Thermal performance of a radial heat sink with longitudinal wavy fins for electronic cooling applications under natural convection," *J. Therm. Anal. Calorim.*, pp. 1–19, Jan. 2022, doi: 10.1007/s10973-021-11162-x/figures/18.
- [8] T. Ambreen, A. Saleem, M. Tanveer, A. K. S. A. Shehzad, and C. W. Park, "Irreversibility and hydrothermal analysis of the MWCNTs/GNPs-based nanofluids for electronics cooling applications of the pin-fin heat sinks: Multiphase Eulerian-Lagrangian modeling," *Case Stud. Therm. Eng.*, vol. 31, p. 101806, Mar. 2022, doi: 10.1016/j.csite.2022.101806.
- [9] R. Ray, A. Mohanty, P. Patro, and K. C. Tripathy, "Performance enhancement of heat sink with branched and interrupted fins," *Int. Commun. Heat Mass Transf.*, vol. 133, p. 105945, Apr. 2022, doi: 10.1016/j.icheatmasstransfer.2022.105945.
- [10] Y. Ding et al., "Experimental and numerical investigation on natural convection heat transfer characteristics of vertical 3-D externally finned tubes," *Energy*, vol. 239, p. 122050, Jan. 2022, doi: 10.1016/j.energy.2021.122050.
- [11] D. Hithaish, V. Saravanan, C. K. Umesh, and K. N. Seetharamu, "Thermal management of Electronics: Numerical investigation of triangular finned heat sink," *Therm. Sci. Eng. Prog.*, vol. 30, p. 101246, May 2022, doi: 10.1016/j.tsep.2022.101246.